Grant Agreement number	17NRM04
Project short name	nPSize
Project full title	Improved traceability chain of nanoparticle size measurements
Deliverable Reference number	**Deliverable 3**
Deliverable Title	**Report on the development and validation of the reference material candidates with non-spherical shape, non-monodisperse size distributions and accurate nanoparticle concentrations**
Lead partner for the Deliverable	LGC
Due Date for Deliverable	July 2021
Actual Date of Submission	October 2021
Coordinator	**Dr Vasile-Dan Hodoroaba** BAM Tel: +40 30 8104 3144 E-mail: Dan.Hodoroaba@bam.de
Project website address	https://www.bam.de/Content/EN/Projects/nPSize/npsize.html
Partners	**LGC**, BAM, LNE, PTB, SMD, VSL, CEA, POLLEN, UNITO

1. Introduction

The aim of work package (WP) 2 was to develop and validate three classes of candidate reference (test) materials (RTMs), with i) well-defined non-spherical shape, ii) relatively high polydispersity index, and iii) accurate particle concentrations.

To fulfil the requirements of the project, 11 different types of materials were prepared (Table 1). Following the initial assessment of the materials suitability, nPSize5_PT_UNITO, nPSize6_AC_UNITO and nPSize7_GN_CEA materials were found unsuitable for the project, due to various reasons. PT material was deemed unsuitable due to its predominantly agglomerated nature. AC material contained relatively high amount of impurities (other particle forms). GN material was found too heterogeneous in both the length and width for the purpose of the project. The remaining 8 candidate RTMs were assessed for their homogeneity and stability and used for successful delivery of the associated activities within the nPSize project.

Table 1. List of the candidate RTMs used in EMPiR nPSize project.

RTM group	Material type	Responsible partner	Material's code	Nominal particle size	Nominal Particle shape
accurate concentration	bimodal gold	LGC	nPSize1_BMG_LGC	30nm and 60nm	spherical
	bimodal gold	LGC	nPSize2_BMG_LGC	30nm and 60nm	spherical
accurate concentration /non-spherical	bipyramidal titania	UNITO/LGC	nPSize3_BPT_UNITO/LGC	60nm lateral x 40nm width	bipyramid
non-spherical	gold cubes	CEA	nPSize4_GC_CEA	60nm x 60nm x 60nm	cube
	platelets titania*	UNITO	nPSize5_PT_UNITO	10-15nm thickness x 50-60nm lateral	platelet
	acicular titania*	UNITO	nPSize6_AC_UNITO	100nm length /15-20nm width; AR 5.5/6	acicular
non-monodispersed /non-spherical	gold nanorods*,	CEA	nPSize7_GN_CEA	10nm width x 20-30nm length	rod
non-monodispersed	monomodal silica, PSD<10%	CEA	nPSize10_MS_CEA	50nm	spherical
	bimodal silica	CEA	nPSize12_BMS_CEA	30nm and 60nm	spherical
	bimodal silica	CEA	nPSize13_BMS_CEA	30nm and 60nm	spherical
	monomodal silica, PSD~20%	CEA	nPSize14_PS_CEA	50nm	spherical

**not included in this report*

This report summarises the outcomes from activities: A2.1.1-A2.1.5, A2.2.1-A2.2.5, A2.3.1-A2.3.5, A2.4.1-A2.4.5 and A2.5.2-A2.5.4 with the focus on the outcomes of homogeneity and stability assessment of the candidate RTMs for the purpose of the nPSize project.

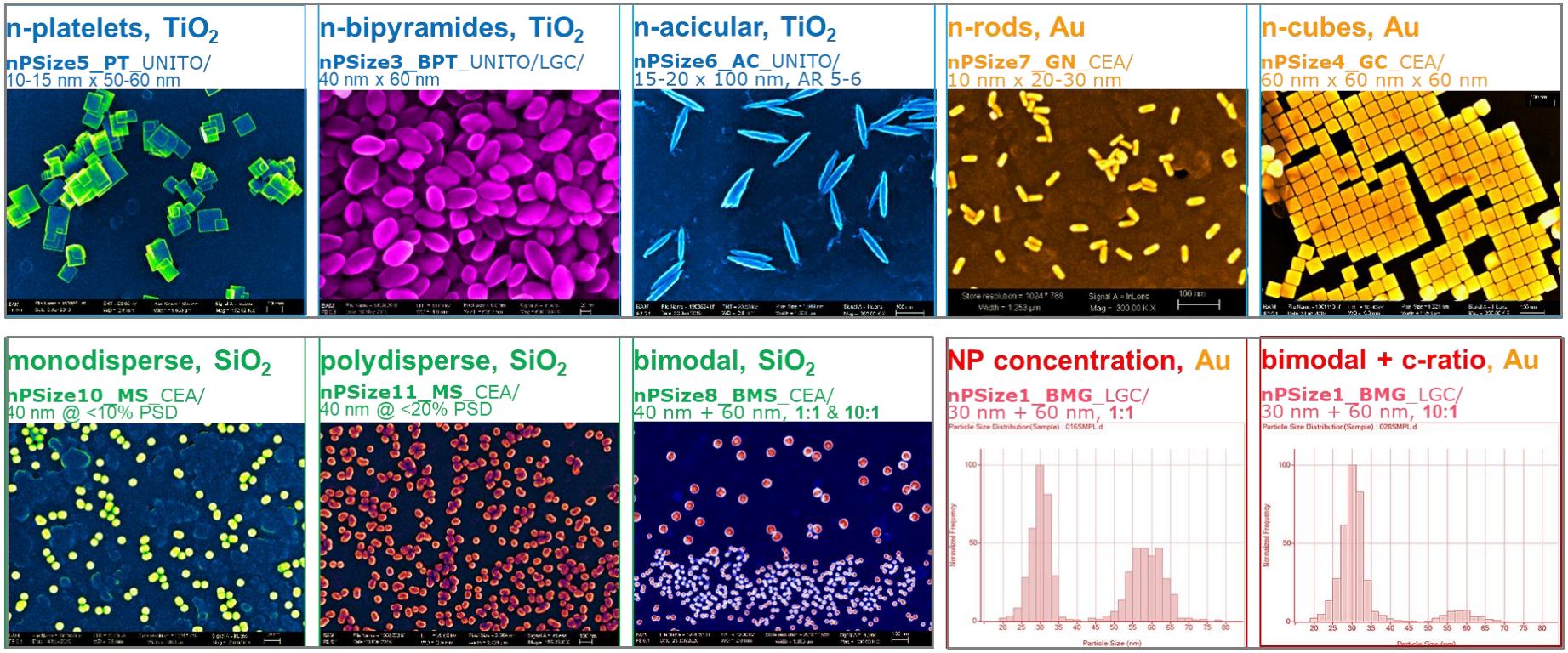

Figure 0. Overview of the various types of nPSize materials.

2. Candidate material preparation and assessment

Bimodal gold (BMG) 'nPSize 1' and 'nPSize 2'

Material preparation: Citrate stabilised colloidal gold suspensions with diameter of approximately 30 nm and 60 nm and dispersed in water were purchased from BBI Solutions Ltd, UK by **LGC**. The two suspensions were gently mixed in 1:1 (nPSize 1) and 1:10 (nPSize 2) ratio (particle number concentration based). The mixed suspension was then gently dispensed into 5.2 ml amber glass vials using an automated process. The vials were sealed under argon. Sealed vials were then sterilised using Co60 gamma irradiation at a minimum dose of 35 kGy. The units were stored at (5 ± 4) °C.

Homogeneity assessment: The homogeneity of the material has been assessed with single particle inductively coupled plasma mass spectrometry (spICP-MS) by **LGC** following frequency approach as described in the methods section below. For this purpose 15 vials were measured in duplicate.

Stability: Samples stored at (5 ± 4) °C were analysed over the duration of the project with spICP-MS (see methods section) by **LGC**. The results showed no significant change in particle number concentration over the tested period.

Pre-Characterisation: The materials were characterised for the particle number concentration in each of the two size fractions by LGC using spICP-MS following either frequency or dynamic mass flow (DMF) approach (see methods section) and for size by **CEA** with TEM (see methods section).

Bipyramid titania (BPT) 'nPSize 3'

Material preparation: Anatase bipyramids with high percentage of {101} facets exposed were synthesized by hydrothermal treatment of Ti(IV)-triethanolammine complex aqueous solution at 423-483 K., as described in details in the literature [1-3] by **UNITO**. The material was dispensed manually into clear 2 ml glass vials and sealed under argon. The units were stored at (5 ± 4) °C.

Homogeneity assessment: The homogeneity of the material has been assessed with total ICP-MS as described in the methods section below by **LGC**. For this purpose, and due to limited number of vials available, 10 vials were measured in duplicate.

Stability: Samples stored at (5 ± 4) °C were analysed over the duration of the project with spICP-MS (see methods section) by **LGC**. The results showed no significant change in particle number concentration over the tested period for the vials filled before December 2018. Significant changes in particle number concentration were observed in vials filled at the later date, caused by the freezing of the mother batch. For this reason, only vials filled before December 2018 were used in the project.

Pre-Characterisation: The material was characterised for the particle number concentration by **LGC** with spICP-MS following DMF approach (see methods section) and for size by **CEA** with TEM (see methods section).

Gold nanocubes (GC) 'nPSize 4'

Material preparation: A suspension of Mono-crystalline colloidal gold cubic nanoparticles were synthesized by **CEA** following the well-known method utilising cetyltrimethylammonium bromide (CTAB), as described in the literature.[4] The materials was kept as single master batches and stored at (5 ± 4) °C.

Homogeneity assessment: Due to practical reasons (high cost and difficulties scaling up) relatively small batch volume (50 ml) of the material was synthesised. Consequently, the material could not be subdivided into a large

number of individual vials/container and between-vials homogeneity could not be studied. The material was kept instead as a single master batch. Small aliquots were taken for the purpose of stability monitoring and characterisation.

Stability: Samples stored at (5 ± 4) °C were analysed over the duration of the project by **CEA** with TEM and SAXS (see the methods section). The results showed no significant change in particle shape and size over the tested period.

Pre-Characterisation: The materials were characterised for the particle size by **CEA** with TEM and SAXS (see methods section).

Monodisperse (MS) 'nPSize 10', polydisperse (PS) 'nPSize 12' and bimodal silica (BMS) 'nPSize 13' and 'nPSize 14'

Material preparation: Several independent batches of colloidal silica particles with nominal particle diameters of either 30 nm or 60 nm were synthesized by **CEA** with PSD varied from < 10% to ~20% following a well-known approach.[5] Monomodal MS and PS materials were used as synthetized whilst BMS materials were obtained following gentle mixing of the 30 nm and 60 nm suspensions in 1:1 (nPSize 13) and 1:10 (nPSize 14) ratio (particle number concentration based). MS, PS and BMS materials were dispensed into 2 ml clear glass vials using an automated process and sealed under argon. The units were stored at room temperature.

Homogeneity assessment: The homogeneity of the material has been assessed with SAXS as described in the methods section below. For this purpose, and due to limited number of vials available, 10 vials were measured in a single analysis batch.

Stability: Samples stored at room temperature were analysed over the duration of the project with SAXS and TEM (see methods section). The results showed no significant change in particle size and relative particle concentration ratio over the tested period.

Pre-Characterisation: The materials was characterised for the particle size and size distribution by **CEA** with TEM (see methods section) and for size and relative particle concentration by **CEA** with SAXS (see methods section).

2.1 Methodology and Instrumentation used for materials homogeneity, stability and pre-characterisation

Total ICP-MS. The analysis was carried out using an Agilent 7700 ICP-MS. The samples were introduced into the plasma via micromist nebuliser, operating at a pumping rate of 0.1 rpm, and using Scott type double pass spray chamber cooled down to 2°C. The instrument was tuned daily for optimum signal intensity and stability with typical operating parameters provided in Table 2.

Table 2. Typical operating parameters of ICP-MS.

Parameter	Agilent 7700
Isotopes measured	^{46,47,48,49}Ti, ^{45}Sc
Integration Time (s)	0.09
Points per spectral peak	3
RF Power (W)	1550
Carrier gas (l min^{-1})	1.15

Make up gas (l min^{-1})	0
Spray Chamber (°C)	2

The ^{46,47,48,49}Ti and ^{45}Sc isotopes were measured in He mode to minimise the interferences. The amount of Ti in the sample was determined by external calibration approach, as described in the previous paragraph. The instrumental blanks and procedural blanks were measured as well and used in results calculation. The limit of detection (LoD) and limit of quantification (LoQ) were calculated using at least 6 blanks in each analytical run. The measurement uncertainty was estimated by combining: measurement repeatability, vial-to-vial variability, average recovery of the quality control material and the specificity obtained by comparing different Ti isotopes. The uncertainty associated with the homogeneity was calculated by combining between unit and within unit components. All results were corrected for the individual dilution factors. Concentrations over the LoQ and corresponding uncertainties are reported in mg kg^{-1} in the ampoules as received. Although four Ti isotopes were measured, only results for isotope 49 are reported since similar values were obtained for all measured isotopes.

spICP-MS. SpICP-MS measurements were performed using an 8900 ICPMS/MS instrument manufactured by Agilent Technologies. The instrument was equipped with micromist nebuliser operating at a pumping rate at 0.1 rpm, Scott type double pass spray chamber cooled to 2 °C, the MassHunter 4.4 (version: G72dC C.01.03) software and microsecond detection capability, allowing analysis in a single particle mode.

The instrument was tuned daily using 1 µgL^{-1} Agilent Tuning solution containing Li, Y and Tl (part: 5190-0465) in order to verify the instrument's performance. Then, the response factor of the instrument to 197Au or 46Ti was optimised with 1 µgkg^{-1} (diluted gravimetrically with 1 mM Na3Ct diluent for Au or with 0.012% (m/m) TEA containing 2 mgL^{-1} NaOH diluent for Ti) of elemental standard (Romil) in order to obtain the best instrument's sensitivity with a minimum background contribution. SpICPMS analysis in fast transient analysis (TRA) mode were performed using a dwell time of 100 µs per point, with no settling time between the measurements and using Single Particle Application Module of the ICPMS MassHunter software (G5714A). For the analysis of gold 'No gas' and a single quad mode was used throughout. In case of Ti, The most abundant Ti isotope, 48Ti was measured in MS/MS mass shift mode, using a reaction cell containing oxygen (O2) and hydrogen (H2) to resolve the polyatomic and isobaric interferences. The first quadrupole (Q1) was set to m/z 48, while the second quadrupole (Q2), separated from Q1 by the octapole reaction cell, was set to m/z 64 (monitored reaction product ion 48Ti16O+). Single Particle Application Module of the ICPMS MassHunter software (G5714A), as well as *in-house* developed Excel spreadsheets, were used for data processing. The instrument was cleaned with Na3Ct or TEA/NaOH diluent after each sample. Each sample was measured 5 times under repeatability conditions. Transport efficiency was determined using the frequency method against LGCQC5050 material (~30 nm nominal gold particles, diluted gravimetrically approximately 4 500 000 times in 1mM Na3Ct buffer) or Dynamic Mass Flow (DMF) method, described elswhere.[6] Particle concentration (C) in the sample was derived from the following equation:

$$C(\mathrm{NP/g}) = \frac{N \cdot Df}{\eta \cdot V} \qquad (1)$$

, where N is the number of particles detected in time scan (NP/min), Df is the sample dilution factor (a.u.) of the samples, η is transport efficiency (a.u.) and V is the sample mass flow (g/min).

TEM. TEM analysis were carried out using a TECNAI OSIRIS (Thermo Fisher Scientific, Eindhoven, Netherlands) transmission electron microscope, equipped with a high sensitivity GATAN camera (BM-Ultra-scan), 2048 x 2048 pixels (Figure).

Figure 1. TECNAI OSIRIS with a high sensitivity GATAN camera.

A cross grating sample ("Calibration gratin Replica" from the company Ted Pella [8]) was used at different magnifications following the calibration procedure defined and integrated in the software by the Thermo Fischer Scientific company.

The different samples made of 'nanoparticles + pure water' were delivered in small watertight tubes. Before the extraction of a drop, the tubes were gently agitated. A 2 µL drop of each diluted suspension was delivered on a copper grid with ultrathin carbon film on a lacey carbon support film (reference: 01824 PELCO) TEM observations. Then, the liquid phase of the drop is evaporated in an exhaust hood. During that process, the nanoparticles are supposed to remain on the ultrathin carbon film of the grid. The grid was then kept under medium vacuum (pressure of a few tenth of Pa) until observations/measurements (that is performed under high vacuum i.e. in the TEM). For the homogeneous deposition of bimodal silica NPs, a new method based on the deposition protocol developed by **BAM** (see D6) with the use of slow evaporation kinetics was implemented in 2021.

The TEM was operated at 200 kV using a typical spot size of "index 5" in order to reduce damaged possibly induced by the beam current.

The typical image size used for nanoparticle measurements is 2048 x 2048 pixels. It is difficult to define a fixed procedure with a defined magnification for the different samples. Indeed, the size and density of the nanoparticles need an adjustment of the magnification in order to optimize the number of nanoparticles in the image versus their size. For example, a too large number of small nanoparticles in the field of vision needs a reduction of the magnification and induces a slight degradation of the resolution or, a small number of NPs in the field leads to a high definition but a large number of images to treat. Here, the method used to determine the dimensional properties of a population of NP by TEM is based on the thresholding tool developed in the frame of the project by **POLLEN** included in the Platypus™ software. At least 100 particles were threshold and particles size distribution of minimum FERET diameter, maximum FERET diameter and diameter base on surface area were provide by the software.

The uncertainty budget associated with the measurement of DNWAE of nanoparticles by TEM first includes: calibration, repeatability, sampling and fitting of the modal value. Moreover, an additional parameter, due to potential measurement bias, is considered when assessing the uncertainty for TEM imaging. Indeed, during the acquisition of TEM images, a bright boundary circles the particle as presented in Figure 2.

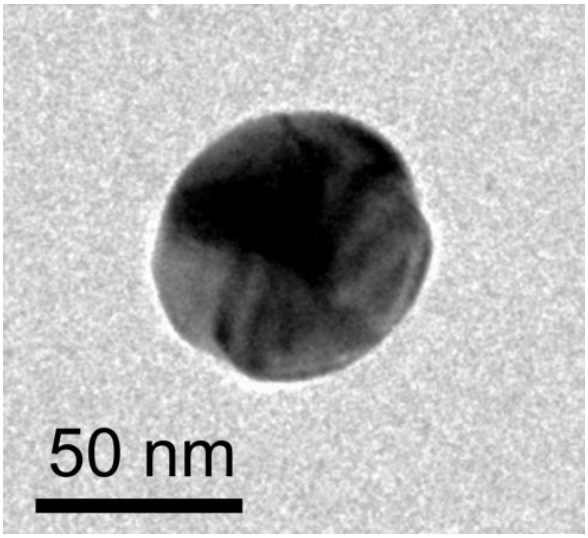

Figure 1. TEM image of a particle of the second mode (60 nm) of the nPSize 1 sample. The thickness of the boundary here is 7 pixels.

This boundary is determined by means of a defocusing of the image by the operator when there is no focusing gradient on the particle. Thus, the contours of the particles on the image appear visually sharper as a result of this defocusing. We can also note that an additional phenomenon may appear when imaging anisotropic or large particles. The white contour may be present on a portion of the particle and is related to the difference in focus because the focal plane does not pass through the entire particle. Moreover, even if the particle is almost spherical, a slight outgrowth (or deformation) above the equatorial plane and/or a slight outgrowth (or deformation) below the equatorial plane can lead to a non-focus contrast in some part of the contour.

The anisotropic particle presented in Figure 2 aims, by its rather caricatural shape, to point out this anisotropic unequal contour contrast described in the sentence before. Indeed, Figure 2 gives a schematic explanation about the different out-of-focus portion of a NP depending on their relative position regarding the focal plan and, the equatorial plan of NP (that is projected on the camera screen).

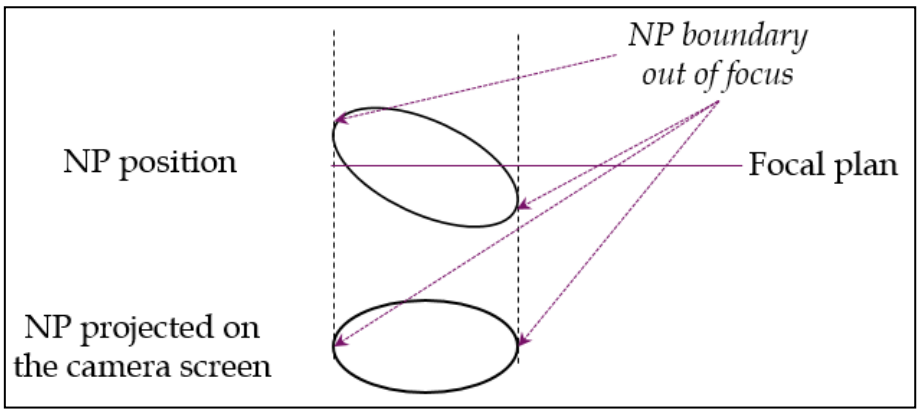

Figure 2. Out-of-focus portion of a NP depending on the position of its equatorial plan regarding the focal plan. The larger the particles and the greater the particle shape anisotropy are, the greater this out-of-focus problem is.

A potential bias induced by the out of focus position must be evaluated for both populations of the sample nPSize 1 (gold nanoparticles). The nominal diameters of both populations as declared by the manufacturer are equal to 30 nm and 60 nm, respectively. On TEM images of nPSize 1 NPs, the thickness variation of the boundary (from the darkest to the brightest part of the boundary) is equal to 6 pixels (the size of a pixel is about 0.41 nm)

and 7 pixels for 30 nm and 60 nm diameter particles, respectively. Because gold NP are near-spherical and as the particle edges are conventionally in between (middle) the brightest and the darkest part of the boundary, the uncertainty related to this boundary, *u(boundary)*, is associated to a uniform distribution and is equal to:

$$u_{boundary} = \frac{a}{\sqrt{3}} \quad (2)$$

, where *a* is the thickness of the bright boundary in nm.

Finally, the composed uncertainty U_{TEM} (k = 1) for the measurement of D_{NWAE} of NP population by TEM is then given by:

$$U_{TEM} = \sqrt{u_{cal}^2 + u_{repeat}^2 + u_{sampling}^2 + u_{fit}^2 + u_{boundary}^2} \quad (3)$$

SAXS. SAXS (Small Angle X-ray Scattering) experiments were carried out on a home design instrument (chemSAXS) at the SWAXS-Lab platform1 (**CEA** Saclay, France). The X-Ray source (8 keV energy Genix from Xenocs) produces a collimated 0.8 mm x 0.8 mm beam on the sample with an incident flux of photons of 1 E8 ph/s. The available q range is 0. 1 nm^{-1} to 3.5 nm^{-1} on the detector (Dectris Pilatus 200K). [4]

Nanoparticle suspensions are placed in glass capillaries or in polyimide (Kapton) sealed tubes (560, icrolumen) of known internal thickness (1.42 ± 0.01 mm). The tubes fabrication extrusion process enables a very good thickness repeatability. Thickness can also be evaluated with a good accuracy measuring water transmission. Samples are placed at the atmospheric pressure. Each SAXS size determination is repeated keeping sample holder, acquisition time, and polyimide tube batch unchanged for both nanoparticle suspension and solvent (water).

SAXS instrument calibration and data correction are done using the state-of-the-art calibration process described by **BAM** (Pauw and Smales). [7]

Data are processed, with the freely available laboratory-made python PySaxs software, which provides data corrections and operations from image averaging to absolute scaling. Mean diameter determination is obtained fitting data with a polydisperse sphere size and Gaussian distribution SAXS model. This model takes into account mean diameter, polydispersity, nanoparticle number concentration, beam convolution, scattering length density of the SiO_2. SAXS data are also processed with MC SAXS, a Monte Carlo algorithm, in order to obtain size distribution being significantly different from Gaussian, especially for polydisperse particles.

2. Results and Discussion

Bimodal gold (BMG) 'nPSize 1' and 'nPSize 2'

Total of 15 ampoules of nPSize1 and nPSize2 were measured in duplicate for the purpose of homogeneity assessment. Material homogeneity assessment was based on the number of particles found per size fraction in each vial of the material (Figure 4), whilst the uncertainty associated with homogeneity was calculated by combining between unit and within unit variability. Particle number-based concentration were calculated with the frequency method against LGCQC5050 material.

For quality control purposes, LGCQC5050 material was submitted to the same sample preparation and measurement procedures as the BMG materials. Recovery rates in the range from 97.3% to 102.7% were obtained, indicating sufficient accuracy of the measurement method.

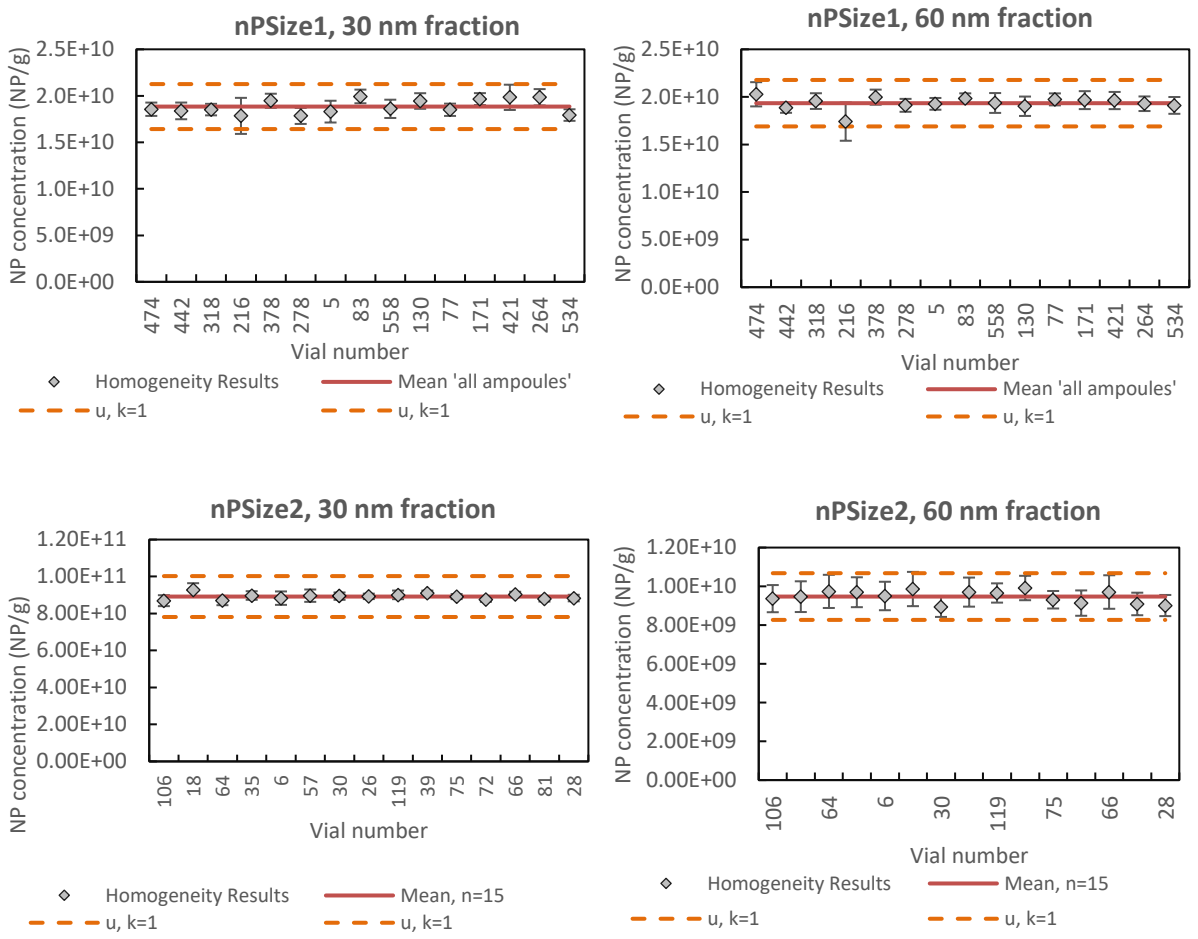

Figure 4. Summary of the homogeneity study on the BMG nPSize1 and nPSize2 materials (error bars associated with data points representing individual vials are stdev from all independent replicate measurements with n=10).

Obtained uncertainty values along with the statistical analysis based on one-way ANOVA (p value) are shown in Table 3. From the statistical analysis it can be concluded that nPSize2 material is homogenous (p in the range of 0.2-0.3 means no significant differences between the tested units were seen), however some inhomogeneity in the 30 nm fraction of the nPSize1 material was observed (p=0.06 is just very close to 0.05 being indicative of significant differences between the vials), but not in the 60 nm fraction (p=0.27). These small differences between the nPSize1 units were attributed to low level of agglomerates formed by the 30 nm particles. Associated measurement uncertainty was calculated in accordance with ISO 17025 and Eurachem/CITAC guidelines and the uncertainty budget is shown below.

Particle number concentrations of 30 nm and 60 nm particle fractions in the BMG materials following the frequency method are shown in Table 4 along with the average ratio of the two size fractions. Associated measurement uncertainty was calculated in accordance with ISO 17025 and Eurachem/CITAC guidelines and the typical uncertainty budget is shown below.

Table 3. Uncertainty associated with the material homogeneity determined by spICPMS (frequency method).

BMG material	30 nm size fraction			60 nm size fraction		
	Standard uncertainty (NP g^{-1})	Relative uncertainty (%)	p* (based on single way ANOVA)	Standard uncertainty (NP g^{-1})	Relative uncertainty (%)	p* (based on single way ANOVA)
nPsize1	7.91E+08	4.2	0.06	7.18E+08	3.7	0.27
nPsize2	2.14E+09	2.4	0.21	3.85E+08	4.0	0.33

**where p < 0.05 indicates significantly different results*

Table 4. Particle number in BMG materials determined by spICPMS (frequency method).

BMG material	30nm size fraction				60nm size fraction				Ratio
	Mean (NP g^{-1})	Standard uncertainty (NP g^{-1})	Expanded uncertainty, k=2 (NP g^{-1})	Relative expanded uncertainty (%)	Mean (NP g^{-1})	Standard uncertainty (NP g^{-1})	Expanded uncertainty, k=2 (NP g^{-1})	Relative expanded uncertainty (%)	(%)
nPsize1	1.9 E10	2.4 E9	4.8 E9	25.7	1.9 E10	2.4 E9	4.9 E9	25.3	1.0
nPsize2	8.9 E10	1.1 E10	2.2 E10	24.8	9.5 E9	1.2 E9	2.4 E9	25.4	9.4

Typical uncertainty budget associated with particle number-based concentration determination with spICPMS 'frequency method':

Within day variability: 3.2%
Between days variability: 4.3%
Transport efficiency: 90.7%
Sample intake: <0.1%
Sample dilution: 1.9%

The nPSize2 material, which was found sufficiently homogenous, was also characterised with the DMF method, which offers direct traceability to the SI unit of kilogram and has lower measurement uncertainties than the frequency approach. [6] For the purpose of DMF, 3 vials of the nPSize 2 material were measured in triplicate. The obtained data are shown in a Table 5 below.

Table 5. Particle number in nPSize2 material determined by spICPMS (DMF method).

BMG material	30nm size fraction				60nm size fraction				Ratio
	Mean (NP g^{-1})	Standard uncertainty (NP g^{-1})	Expanded uncertainty, k=2 (NP g^{-1})	Relative expanded uncertainty (%)	Mean (NP g^{-1})	Standard uncertainty (NP g^{-1})	Expanded uncertainty, k=2 (NP g^{-1})	Relative expanded uncertainty (%)	(%)
nPsize2	9.1 E10	0.4 E10	0.9 E10	9.5	9.7 E9	0.7 E9	1.5 E9	15.0	9.4

Typical uncertainty budget associated with particle number-based concentration determination with spICPMS 'frequency method':

	30nm fraction	***60nm fraction***
Within day variability:	32.6%	61.1%
Between days variability:	48.7%	28.1%
Transport efficiency:	18.1%	10.4%
Sample intake:	<0.1%	<0.1%
Sample dilution:	0.6%	0.4%

Both materials were found stable in terms of the number-based concentration over the tested period with no significant difference seen (within k=1, being ~13%) between measurements.

Both materials were also found stable in terms of particle size and size distribution over the tested period based on the TEM measurement conducted in October 2019, January 2020 and March 2021. For the purpose of TEM, thresholding was performed on 5 images for 128 labelled particles in October 2019, on 16 images for 222 labelled particles in January 2020 and on 17 images for 215 particles labelled in March 2021. TEM measurements of nPSize2 conducted in September 2019 and March 2021. Thresholding was performed on 17 images for 101 labelled particles in September 2019 and on 18 images for 228 particles labelled in March 2021.

Figure 5 shows representative TEM images of nPSize 1and nPSize2. The equivalent area diameter (D_{ae}) results with mean diameter, median diameter and mode are summarized in Table 6.

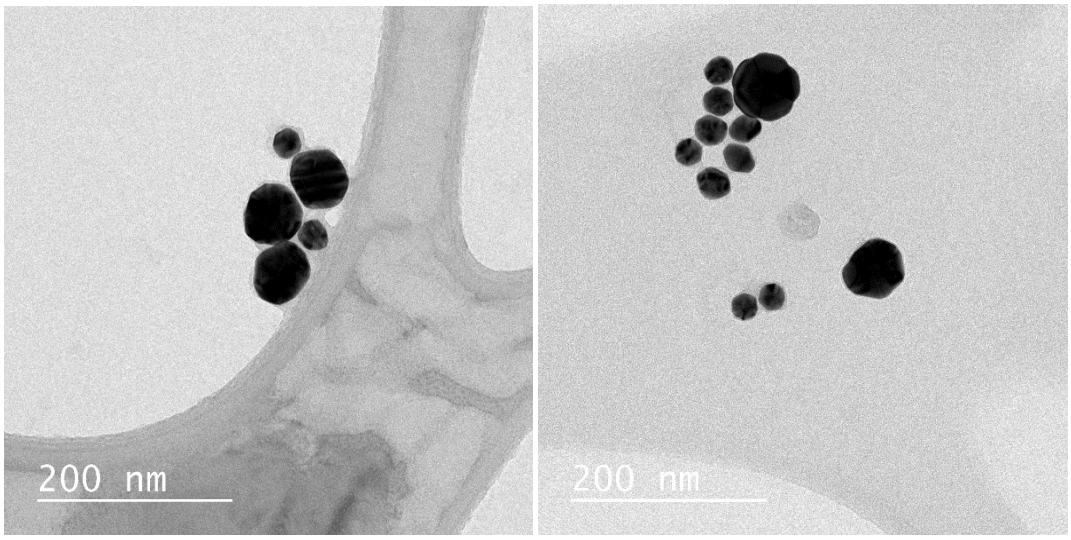

Figure 5. Representative TEM images of nPSize1 (left) and nPSize2 (right).

Table 6. Summary of TEM stability and pre-characterisation results obtained for nPSize 1 and nPSize 2 materials.

Date	nPSize1						nPSize2					
	Mode 1			Mode 2			Mode 1			Mode 2		
	$D_{AE\ (nm)}$			$D_{AE\ (nm)}$			$D_{AE\ (nm)}$			$D_{AE\ (nm)}$		
	mean	mode	med.	mean	mode	med.	mean	mode	med.	mean	mode	med.
2019	61.8	56.1	62.2	31.1	31.9	30.7	63.1	62.8	63.0	30.9	32.8	31.8
2020	61.6	57.1	61.4	30.5	29.4	30.5	-	-	-	-	-	-
2021	62.2	62.9	62.4	30.8	31.1	31.2	61.7	63.0	61.8	31.1	31.3	30.8
Mean ± u, k=1	**61.9 ± 0.5**	**58.7± 3.7**	**62.0± 2.0**	**30.8 ± 0.5**	**30.8 ± 1.3**	**30.8 ± 0.5**	**62.4 ± 1.0**	**62.9 ± 0.5**	**62.4 ± 0.8**	**31.0 ± 0.5**	**32.1 ±1.1**	**31.3 ±0.7**

Bipyramid titania (BPT) 'nPSize 3'

For the purpose of homogeneity, a total of 10 ampoules of BPT were measured in duplicate. The values obtained for each ampoule, as well as the average amount of titanium in the BPT material are shown in Table 7 and Figure 6, with their associated measurement uncertainty calculated in accordance with ISO 17025 and Eurachem/CITAC guidelines. LoQ of 7.01 mg kg^{-1} was achieved.

Total amount of titanium in the BPT material was measured with ICP-MS using external calibration approach, obtaining the mean of 2560 mg kg^{-1} with the relative expanded measurement uncertainty of 5%. The material was found homogenous (F = 1.03, p = 0.48 based on a single way ANOVA) with the associated relative standard uncertainty of 2%. The uncertainty associated with homogeneity was calculated by combining between unit and within unit variability, obtaining standard uncertainty of 45 mg kg^{-1}, or relative standard uncertainty of 2%.

Table 7. Amount of titanium in BPT material.

Ampoule number	Titanium (mg kg^{-1})			
	Mean (mg kg^{-1})	Standard uncertainty (mg kg^{-1})	Expanded uncertainty, k=2 (mg kg^{-1})	Relative expanded uncertainty (%)
0003	2505	75	150	6
0004	2585	69	139	5
0007	2582	70	140	5
0008	2519	59	119	5
0010	2576	76	153	6
0012	2518	65	130	5
0013	2622	82	164	6
0015	2566	74	148	6
0017	2593	65	131	5
0021	2504	64	128	5
Average BPT material	**2560**	**60**	**121**	**5**

The uncertainty budget is shown below:

Repeatability:	20.2%
Between vial variability:	2.4%
Recovery:	76.6%
Specificity:	0.8%

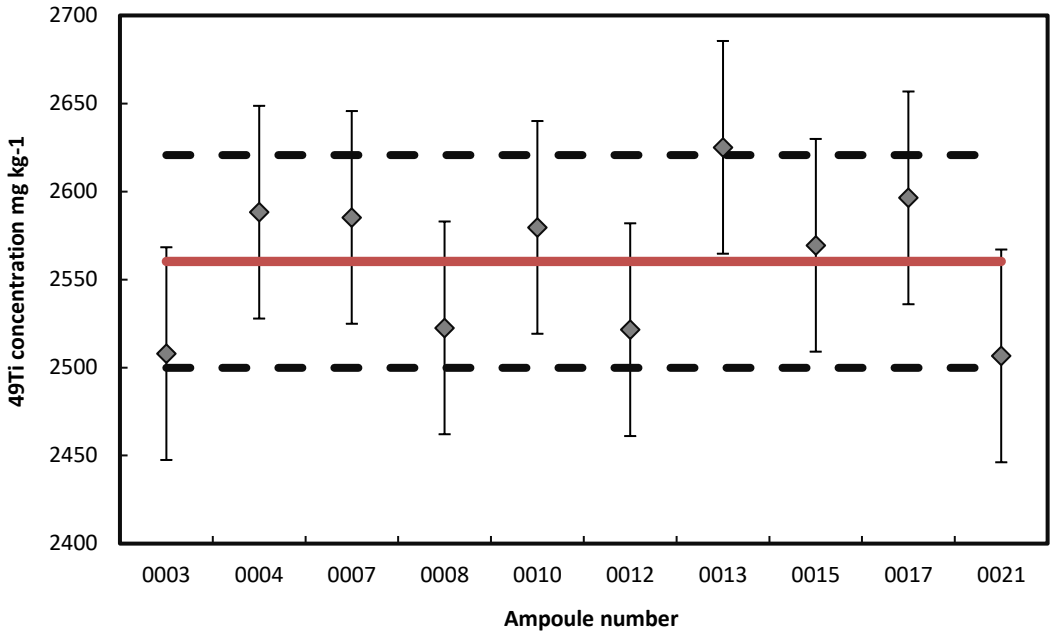

Figure 6. Summary of the homogeneity assessment of the BPT material.

For quality control purposes, ionic Ti standard from NIST was submitted by **LGC** to the same sample preparation and measurement procedures as the BPT material. Recovery rates in the range from 98.8% to 102.9% were obtained. In addition to these spiking experiments were performed to check for possible matrix effects by adding ionic titanium to the BPT samples. In this case recoveries in the range from 92.1% to 97.4% were obtained, suggesting no significant matrix effects.

Table 8. Particle number-based concentration in BPT material.

Material	Particle number			
	Mean (NP g^{-1})	Standard uncertainty (NP g^{-1})	Expanded uncertainty, k=2 (NP g^{-1})	Relative expanded uncertainty (%)
BPT nPSize3	1.08 E13	5.49 E11	1.10 E12	10.2

Total of 9 ampoules of BPT material were measured in triplicate over three days with spICPMS using DMF method for TE determination.[6] Obtained particle number is shown in Table 8 with associated measurement uncertainty calculated in accordance with ISO 17025 and Eurachem/CITAC guidelines. Typical uncertainty budget is shown in the next table.

Typical uncertainty budget associated with particle number-based concentration determination with spICPMS (DMF method):

Within day variability:	54.5%
Between days variability:	17.8%
Transport efficiency:	27.1%
Sample intake:	<0.1%
Sample dilution:	0.6%

Material stability testing was based on the particle number found in the individual ampoules using spICPMS with particle frequency method for TE determination. Summary of the obtained data is shown in Figure 7 and 8. Data points represent an average of two independent preparations per vial, each measured five times under repeatability conditions.

Error bars are stdev from these measurements (n=10). Data marked in black 'Bipy new vial @2018' is the BPT material from the first shipment received at **LGC** in 2018 where the tested vials were opened on the day of the measurements (Jan 2020), 'Bipy old vial @2018' also come from the first shipment received in 2018 but these vials were previously opened (Jan-Apr 2019) and stored in the fridge covered with parafilm. 'Bipy stock' is the BPT suspension received at LGC in 2018 stored in the large glass vial with septum cap in the fridge, which is an aliquot taken directly by **UNITO** from the master batch 01, whilst 'Bipy new vial @2019' represent vials received at LGC in 2019 (ampouled by **UNITO** in 2019) opened on the day of analysis (Jan 2020). Data show that only 'Bipy stock' and previously unopened vials that come from the BPT ampouled at **UNITO** in 2018 are stable and give the particle number-based concentration in agreement with the DMF characterisation data (see previous paragraph) obtained in April 2019. Low particle number-based concentration in the remaining samples can be attributed to particle aggregation/aggregation (data not shown). As later identified by the material producer, observed instability was caused by the accidental exposure of the master batch/vials to temperatures below freezing at **UNITO**. Deagglomeration strategy involving 1h bath sonication in conjunction with heating to 60°C was tested, but such efforts were proven unsuccessful as shown in Figure 8.

All Partners were given recommendation to only use vials ampouled and shipped in 2018 for their measurements (enough has been produced by **UNITO** to support the remaining activities under the nPSize project).

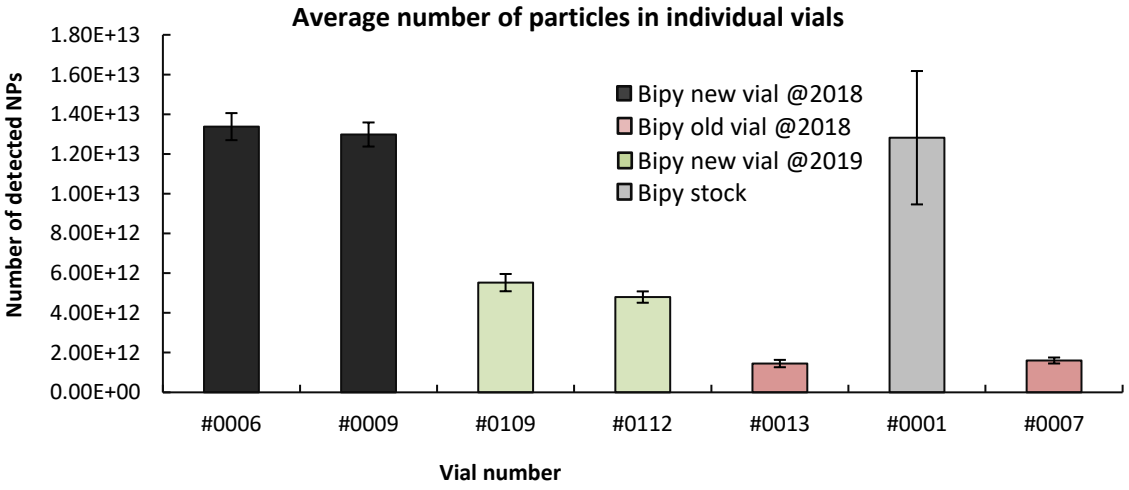

Figure 7. Summary of the particle number-based concentration measured with spICPMS (frequency method) in the BPT material.

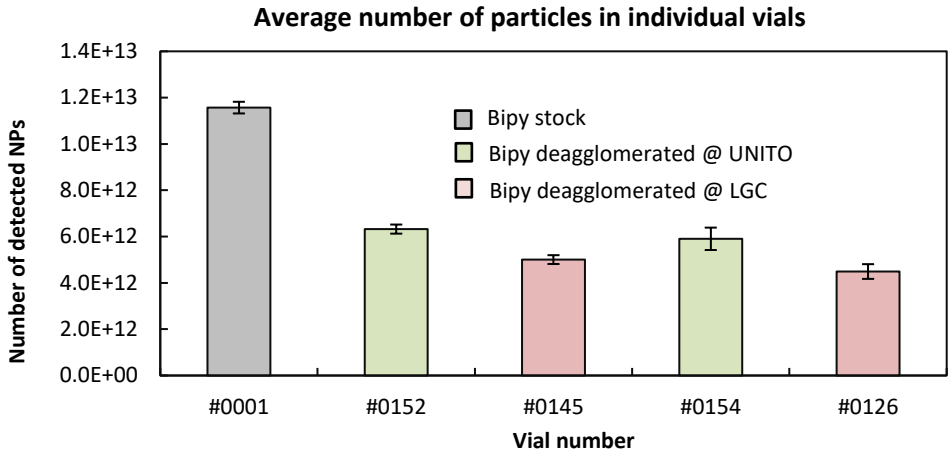

Figure 8. Summary of the particle number-based concentration measured with spICPMS (frequency method) in the BPT material.

BPT material was also measured by TEM in October 2019, January 2020 and March 2021. Thresholding was performed on 17 images for 124 labelled particles in October 2019, on 14 images for 104 labelled particles in January 2020 and on 8 images for 117 particles labelled in March 2021. Figure 9 shows an image of nPSize 3. The minimum FERET diameter ($D_{minFeret}$) and maximum FERET diameter ($D_{maxFeret}$) results with mean diameter, median diameter and mode are summarized in **Error! Reference source not found.**.

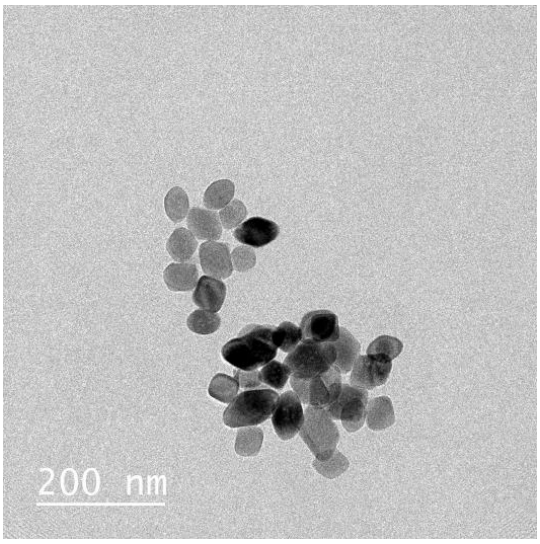

Figure 9. Representative TEM image of nPSize3.

Table 9. Summary of TEM stability and pre-characterisation results obtained for nPSize3 material.

Date	nPSize 3					
	$D_{minFeret\ (nm)}$			$D_{maxFeret\ (nm)}$		
	mean	mode	med.	mean	mode	med.
2019	45.5	44.8	45.3	64.3	64.1	65.0
2020	44.5	44.3	44.3	57.9	52.6	56.2
2021	45.7	44.3	45.0	55.6	50.0	53.5
Mean ± u, k=1	**45.2 ± 0.6**	**44.5 ± 0.3**	**44.9 ± 0.5**	**59.3 ± 4.5**	**55.6 ± 7.5**	**58.2 ± 6.0**

Gold nanocubes (GC) 'nPSize 4'

As already explained in the previous section the material's between unit homogeneity could not be studies as only a small single batch was obtained for the purpose of the project.

Material was measured with TEM in September 2019 and March 2020. Thresholding was performed on 31 images for 104 labelled particles in September 2019 and on 14 images for 108 labelled particles in March 2020. **Error! Reference source not found.** 10 shows an image of nPSize4. The minimum FERET diameter ($D_{minFeret}$) and maximum FERET diameter ($D_{maxFeret}$) results with mean diameter, median diameter and mode are summarized in **Error! Reference source not found.**.

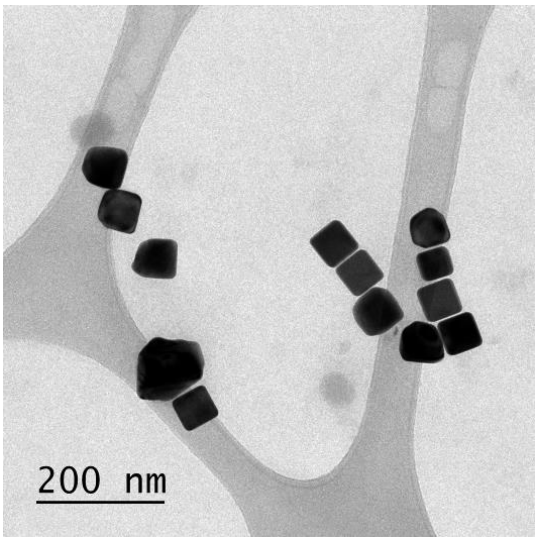

Figure 10. Representative TEM image of nPSize4.

Table 10. Summary of TEM stability and pre-characterisation results obtained for nPSize4 material.

Date	nPSize4					
	$D_{minFeret}$ (nm)			$D_{maxFeret}$ (nm)		
	mean	mode	med.	mean	mode	med.
2019	58.8	58.4	58.7	62.1	60.3	61.2
2020	59.1	57.1	59.1	61.4	57.9	60.9
Mean ± u, k=1	59.0 ± 0.5	57.8 ± 0.9	58.9 ± 0.5	61.8 ± 0.5	59.1 ± 1.7	61.1 ± 0.5

Monodisperse (MS) 'nPSize 10', polydisperse (PS) 'nPSize 12' and bimodal silica (BMS) 'nPSize 13' and 'nPSize 14'

Homogeneity of the nPSize10, nPSize12, nPSize13 and nPSize14 was assessed with SAXS based on the measurements performed on 10 individual vials from each of the materials. The summary of the obtained results (SAXS curves) is shown in Figure 11. No differences between units were seen and the materials were considered sufficiently homogeneous based on the SAXS data.

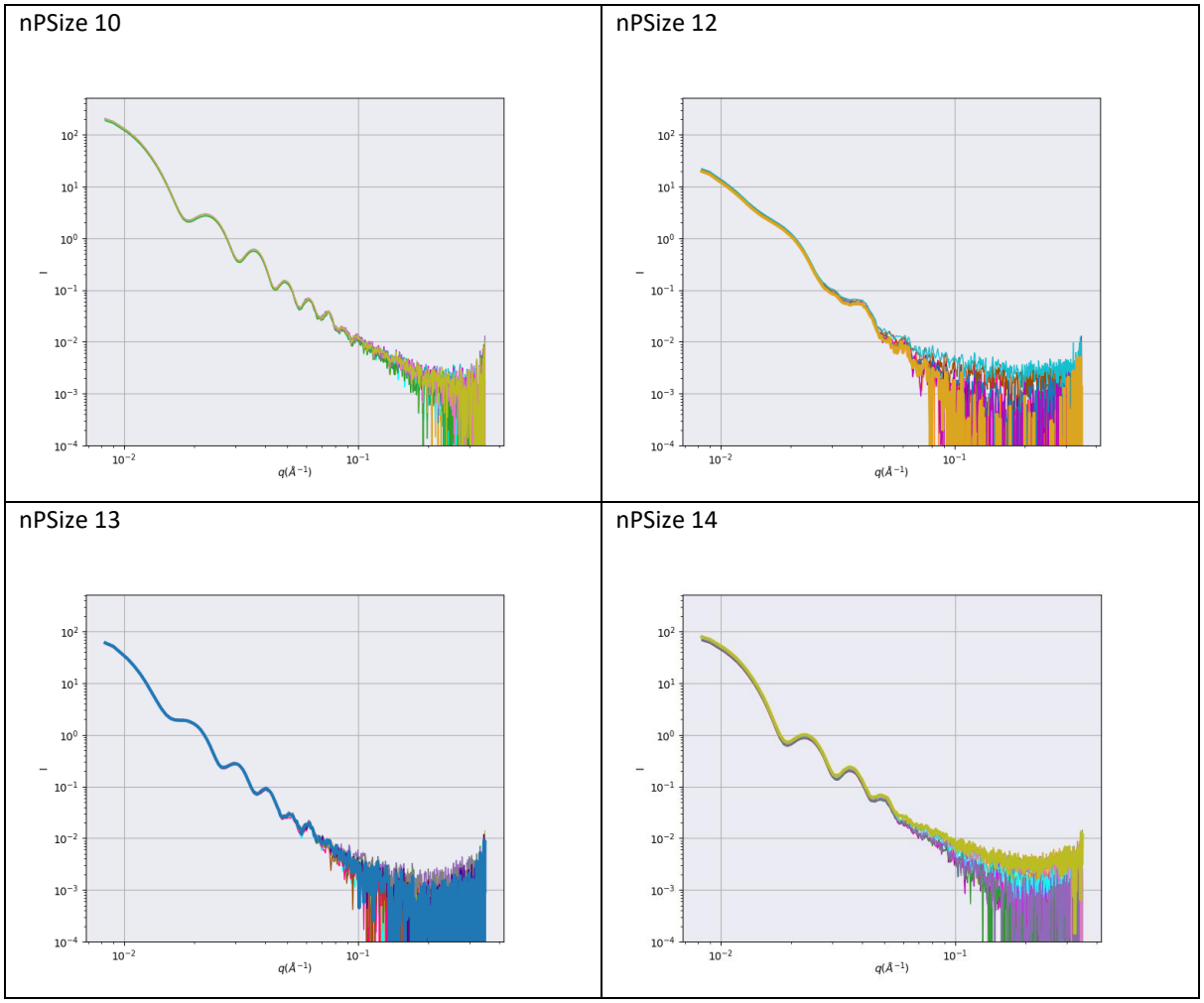

Figure 11. Summary of homogeneity assessment of the MS, PS and BMS materials. Individual colours represent overlaid SAXS curves derived from measurements performed on 10 independent vials of each of the materials.

SAXS was also used to assess the materials stability upon storage. No significant differences were found in the particle size, size distribution and number concentration in the silica materials. The summary of data obtained for the nPSize10 material is shown in Table 11 as an example. Similar results were obtained for the nPSize14 material but are not shown in this report.

Table 11. Summary of SAXS stability results obtained for nPSize10 material.

Date	Diameter (nm)	Sigma	Concentration (NP cm^{-3})
2019-01-11	50.85	1	1.29E+13
2019-11-05	50.55	1.8	1.47E+13
2020-01-29	50.91	2.27	1.31E+13
2020-06-19	50.48	1.99	1.91E+13
2021-01-06	50.54	0.79	1.68E+13
2021-03-18	50.59	2.1	1.80E+13
2021-05-20	49.74	2.1	2.00E+13
2021-08-02	50.14	2.8	1.85E+13

Silica materials were also found stable in terms of particle size and size distribution over the tested period based on the TEM measurement conducted in March 2020 and January 2021. For nPSize10, thresholding was performed on 5 images for 125 labelled particles in March 2020 and on 9 images for 142 particles labelled in January 2021. For nPSize14, thresholding was performed on 9 images for 177 labelled particles in September 2020 and on 11 images for 106 particles labelled in January 2021. Figure 5 shows representative TEM images of nPSize10 and nPSize14. The equivalent area diameter (D_{ae}) results with mean diameter, median diameter and mode are summarized in Table 12.

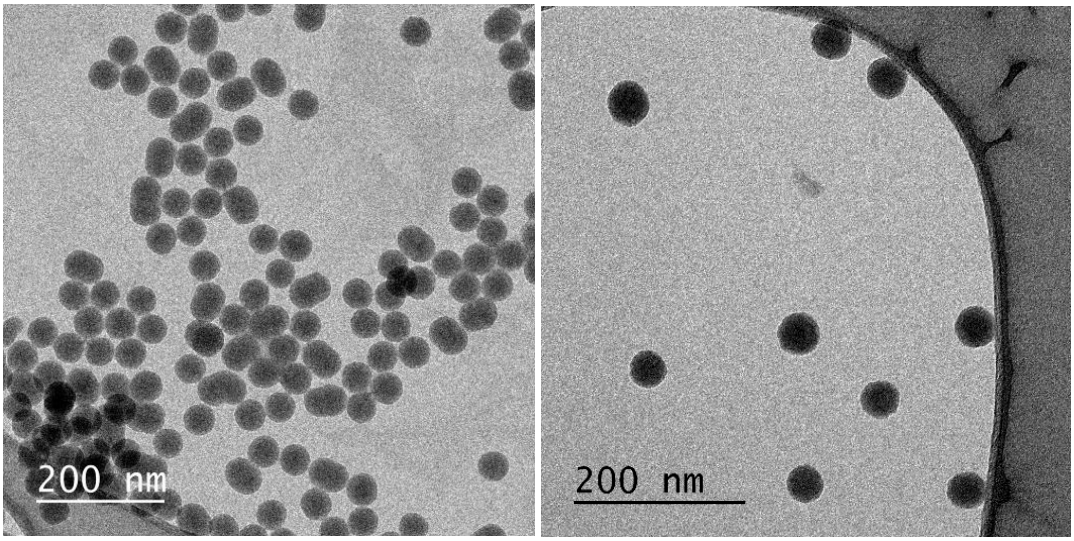

Figure 12. Representative TEM images of nPSize10 (left) and nPSize14 (right).

Table 12. Summary of TEM stability and pre-characterisation results obtained for nPSize10 and nPSize14 materials.

Date	$D_{AE\,(nm)}$					
	nPSize10			nPSize14		
	mean	mode	med.	mean	mode	med.
2020	48.3	48.8	48.3	47.1	47.7	47.4
2021	50.1	50.4	49.5	48.3	47.1	48.1
Mean ± u, k=1	**49.2 ± 1.3**	**49.6 ± 1.1**	**48.9 ± 0.8**	**47.7 ± 0.8**	**47.4 ± 0.4**	**47.8 ± 0.5**

The summary of the results obtained by SAXS for the BMS, nPSize12 and nPSize13, materials is shown in Figure 13. In case of the BMS materials, data analysis was performed using the Monte-Carlo method to estimate the particle size distributions.

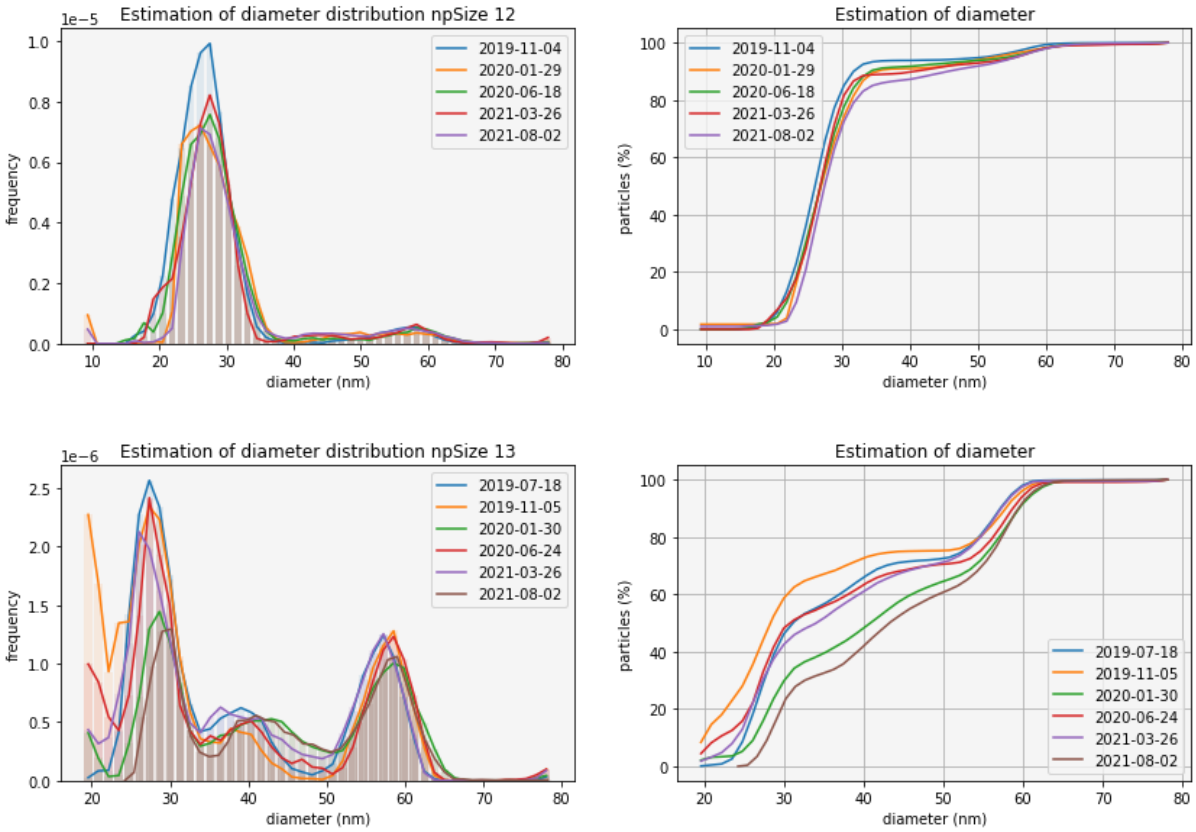

Figure 13. Summary of SAXS stability results obtained for BMS, nPSize13 and nPSize14, materials.

For the nPSize13 material, TEM thresholding was performed on 10 images for 149 labelled particles in September 2020 and on 17 images for 200 particles labelled in March 2021. In case of the nPSize13, thresholding was performed on 8 images for 127 labelled particles in September 2020 and on 14 images for 224 particles labelled in March 2021. **Error! Reference source not found.** shows an image of nPSize12 and nPSize13. The equivalent area diameter (D_{ae}) results with mean diameter, median diameter and mode are summarized in **Error! Reference source not found.**.

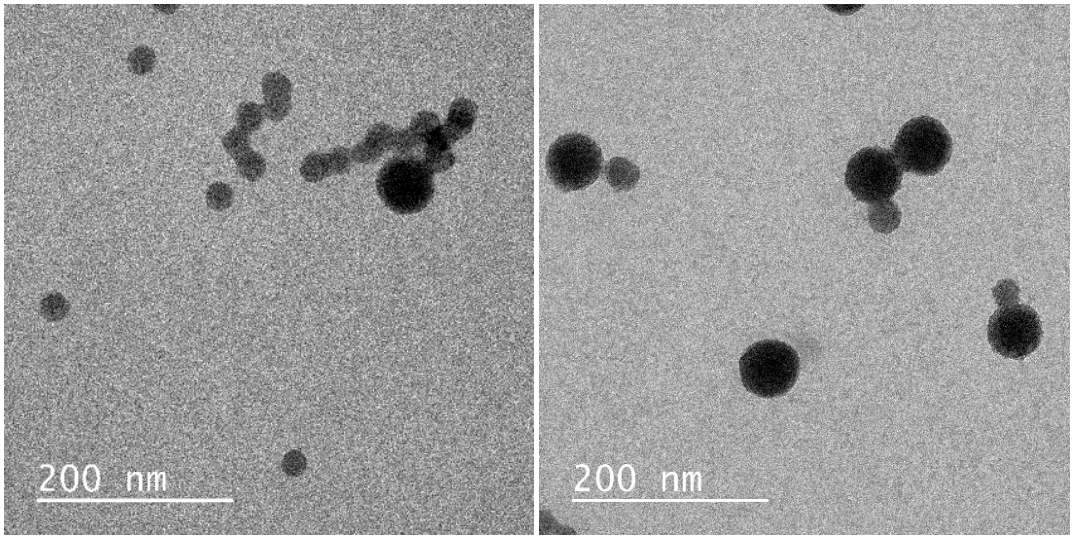

Figure 14. Representative TEM images of nPSize12 (left) and nPSize13 (right).

Table 13. Summary of TEM stability and pre-characterisation results obtained for nPSize12 and nPSize13 materials.

Date	nPSize12						nPSize13					
	Mode 1			Mode 2			Mode 1			Mode 2		
	$D_{AE\ (nm)}$			$D_{AE\ (nm)}$			$D_{AE\ (nm)}$			$D_{AE\ (nm)}$		
	mean	mode	med.	mean	mode	med.	mean	mode	med.	mean	mode	med.
2020	29.5	28.9	29.5	58.0	57.6	58.4	28.1	28.7	28.2	58.2	57.8	58.1
2021	29.4	30.2	29.6	57.7	57.4	57.4	29.6	30.2	30.2	59.2	59.7	59.3
Mean ± u, k=1	**29.5 ± 0.5**	**29.6 ± 0.9**	**29.6 ± 0.5**	**57.9 ± 0.5**	**57.5 ± 0.5**	**57.9 ± 0.7**	**28.9 ± 1.1**	**29.5 ± 1.1**	**29.2 ± 1.4**	**58.7 ± 0.7**	**58.8 ± 1.3**	**58.7 ± 0.8**

The cumulate curves derived from TEM data, **Error! Reference source not found.**, give a proportion of the first population ca. 85% for nPSize12 and ca. 54% for nPSize13.

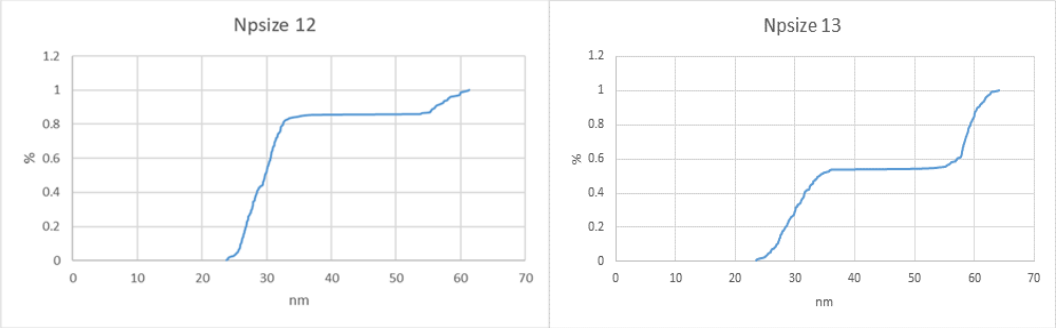

Figure 15. Cumulate curves of nPSize12 (left) and nPSize13 (right).

3. Conclusions

Based on the homogeneity, stability and pre-characterisation data obtained on the nPSize1 to nPSize14 materials and shown in this report, materials, nPSize1, nPSize2, nPSize3, nPSize4, nPSize7, nPSize10, nPSize12, nPSize13 and nPSize14 were found to be suitable candidate RTMs for the use in the EMPiR nPSize project.

References:

[1] Pellegrino, F.; Isopescu, R.; Pellutie, L.; Sordello, F.; Rossi, A. M.; Ortel, E.; Martra, G.; Hodoroaba, V. D.; Maurino, V., Machine learning approach for elucidating and predicting the role of synthesis parameters on the shape and size of TiO2 nanoparticles. *Sci Rep* 2020, 10 (1), 18910.

[2] Mino, L.; Pellegrino, F.; Rades, S.; Radnik, J.; Hodoroaba, V.-D.; Spoto, G.; Maurino, V.; Martra, G., Beyond Shape Engineering of TiO2 Nanoparticles: Post-Synthesis Treatment Dependence of Surface Hydration, Hydroxylation, Lewis Acidity and Photocatalytic Activity of TiO2 Anatase Nanoparticles with Dominant {001} or {101} Facets. *ACS Applied Nano Materials* 2018, 1 (9), 5355-5365.

[3] Sordello, F.; Pellegrino, F.; Prozzi, M.; Minero, C.; Maurino, V., Controlled Periodic Illumination Enhances Hydrogen Production by over 50% on Pt/TiO2. *ACS Catal* 2021, 11 (11), 6484-6488.

[4] Deumer, J., Pauw, B. R., Marguet, S., Skroblin, D., Taché, O., Krumrey, M., & Gollwitzer, C. (2021). Small-angle X-ray scattering: characterization of cubic Au nanoparticles using Debye's scattering formula. *arXiv preprint* arXiv:2109.06570.

[5] Stöber, W., Fink, A. and Bohn, E., Controlled growth of monodisperse silica spheres in the micron size range. *Journal of colloid and interface science*, 1968, 26(1), 62-69.

[6] Cuello-Nuñez, S., Abad-Álvaro, I., Bartczak, D., del Castillo Busto, M.E., Ramsay, D.A., Pellegrino, F. and Goenaga-Infante, H., The accurate determination of number concentration of inorganic nanoparticles using spICP-MS with the dynamic mass flow approach. *Journal of Analytical Atomic Spectrometry*, 2020, 35(9), 1832-1839.

[7] Glen J. Smales and Brian R. Pauw 2021 *JINST* 16 P06034.

[8] https://www.tedpella.com/Calibration_html/TEM_STEM_Test_Specimens.htm.aspx